J. Anat. (1999) **194**, pp. 463–471, with 6 figures Printed in the United Kingdom

Dynamic injury tolerances for long bones of the female upper extremity

STEFAN M. DUMA[1], PHIL H. SCHREIBER[1], JOHN D. McMASTER[2], JEFF R. CRANDALL[1], CAMERON R. BASS[1], WALTER D. PILKEY[1]

[1] *Automobile Safety Laboratory, University of Virginia, Charlottesville, Virginia, USA, and* [2] *Department of Orthopaedic and Accident Surgery, University Hospital, Queen's Medical Centre, Nottingham, UK*

(*Accepted 12 January 1999*)

ABSTRACT

This paper presents the dynamic injury tolerances for the female humerus and forearm derived from dynamic 3-point bending tests using 22 female cadaver upper extremities. Twelve female humeri were tested at an average strain rate of 3.7 ± 1.3 %/s. The strain rates were chosen to be representative of those observed during upper extremity interaction with frontal and side airbags. The average moment to failure when mass scaled for the 5th centile female was 128 ± 19 Nm. Using data from the in situ strain gauges during the drop tests and geometric properties obtained from pretest CT scans, an average dynamic elastic modulus for the female humerus was found to be 24.4 ± 3.9 GPa. The injury tolerance for the forearm was determined from 10 female forearms tested at an average strain rate of 3.94 ± 2.0 %/s. Using 3 matched forearm pairs, it was determined that the forearm is 21 % stronger in the supinated position (92 ± 5 Nm) versus the pronated position (75 ± 7 Nm). Two distinct fracture patterns were seen for the pronated and supinated groups. In the supinated position the average difference in fracture time between the radius and ulna was a negligible 0.4 ± 0.3 ms. However, the pronated tests yielded an average difference in fracture time of 3.6 ± 1.2 ms, with the ulna breaking before the radius in every test. This trend implies that in the pronated position, the ulna and radius are loaded independently, while in the supinated position the ulna and radius are loaded together as a combined structure. To produce a conservative injury criterion, a total of 7 female forearms were tested in the pronated position, which resulted in the forearm injury criterion of 58 ± 12 Nm when scaled for the 5th centile female. It is anticipated that these data will provide injury reference values for the female forearm during driver air bag loading, and the female humerus during side air bag loading.

Key words: Skeletal injury; bone fractures; automobile safety; air bags.

INTRODUCTION

Although air bags have reduced the risk of fatal injuries in automobile collisions, they have increased the incidence of some nonfatal injuries including upper extremity injuries. It is suggested that there may be a 40 % increase in risk of serious upper extremity injury to belted occupants with air bags versus those without air bags (NHTSA, 1996). Kuppa et al. (1997) showed that 1.1 % of drivers who were restrained only by a seat belt experienced an upper extremity injury, versus 4.4 % of drivers in the presence of a deploying air bag. Although air bag depowering is expected to have a beneficial effect on the frequency of upper extremity injuries from air bags, the injury tolerances of the humerus and forearm must be known in order to design driver and side air bags that minimise the risk of serious injury to the upper limbs.

Given that female bones in general have a lower mineral content and are thus weaker than male bones, the injury tolerance for small females provides a conservative estimate for the general driving population. Several papers have addressed the humerus bending strength and the results are summarised in Table 1. All previous experiments were performed under quasistatic conditions. It has been shown that

Correspondence to Mr Stefan M. Duma, Automobile Safety Laboratory, University of Virginia, 1011 Linden Avenue, Charlottesville, Virginia 22902, USA.

Table 1. *Published humerus tolerance data*

S	Y	MBF	FBF
Weber (1859)	1859	115	73
Messerer (1880)	1880	151	85
Kirkish et al. (1996)	1996	155±45*	84
	Scaled	230 (50th percentile)**	134 (5th percentile)
Kallieris et al. (1997)	1997	138±9	

S, study; Y, year; MBF, male bending failure (Nm); FBF, female bending failure (Nm).
*± indicates standard deviation, otherwise only one test was conducted; ** indicates data mass scaled to the given centile male or female respectively.

the strength of bone increases with increased strain rate (Carter & Caler, 1983). This indicates that the previous studies underestimate the strength of bone in a dynamic environment. Moreover, the studies by Weber (1859) and Messerer (1880) are dated and involve sample populations that are likely to be different from modern populations. Kallieris et al. (1997) performed tests involving only males, while Kirkish et al. (1996) tested only 1 female. The current study addresses the lack of recent dynamic tests with female humeri.

The risk of injury to the forearm from the driver side air bag has been investigated. Bass et al. (1997) compared air bag tests with cadaveric upper extremities with matched tests using the SAE fully instrumented 5th centile female upper extremity. They found that a forearm moment of 67 Nm in the dummy corresponded to a 50% risk of at least 1 fracture in the radius and ulna. However, no direct dynamic bending moment tests on female forearms were undertaken in that study. Furthermore, while quasi-static tests have been performed on the radius and ulna separately, no published dynamic tolerance data exist for the intact female forearm. An additional goal of the forearm test series was to determine the difference in dynamic bending strength between supinated and pronated forearms. In the supinated position, the radius and ulna are essentially parallel to each other, whereas in the pronated position, the distal radius rotates over the ulna and brings the radius above and across the ulna. The purpose of this study was to determine the dynamic bending strengths of the female humerus and forearm, and to investigate the relationship between forearm strength and radius and ulna orientation.

MATERIALS AND METHODS

Humerus tests

Twelve female humeri were prepared by disarticulating the upper extremity at the shoulder and elbow joints. As shown in Table 2, the average age of these specimens was 57±11 y with an average body mass of 58.7±7.6 kg. The age limit was set below 70 y in order to represent the weakest group of automobile occupants, while excluding the older occupants which constitute a very small portion of the driving population. Enough soft tissue was removed from each humerus to expose 50 mm of bone at the distal and proximal ends. The exposed ends were potted in epoxy putty (Protective Coating Co., PC-7) to a depth of 30 mm using removable moulds. Simple support fixtures were attached to the hardened epoxy as shown in Figure 1. The support fixtures acted in the same manner as rollers. Strain gauges (Micro Measure-

Table 2. *Specimen information for female humerus tests*

T	SA	A	BM	CD
1.1	79 right	54	71.1	Myocardial infarction
1.2	79 left	54	71.1	Myocardial infarction
1.3	75 right	59	64.4	Congestive heart failure
1.4	75 left	59	64.4	Congestive heart failure
1.5	78 right	41	56.0	Ovarian carcinoma
1.6	78 left	41	56.0	Ovarian carcinoma
1.7	82 right	50	49.1	Breast and liver carcinoma
1.8	82 left	50	49.1	Breast and liver carcinoma
1.9	81 right	74	52.7	Breast carcinoma
1.10	81 left	74	52.7	Breast carcinoma
1.11	80 right	66	59.0	Lung carcinoma
1.12	80 left	66	59.0	Lung carcinoma

T, test; SA, subject aspect; A, age (years); BM, body mass (kg); CD, cause of death.

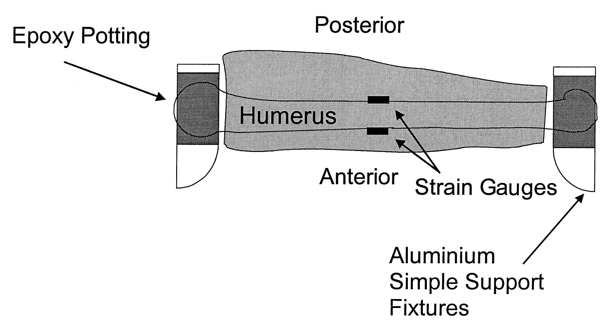

Fig. 1. Humerus preparation and instrumentation.

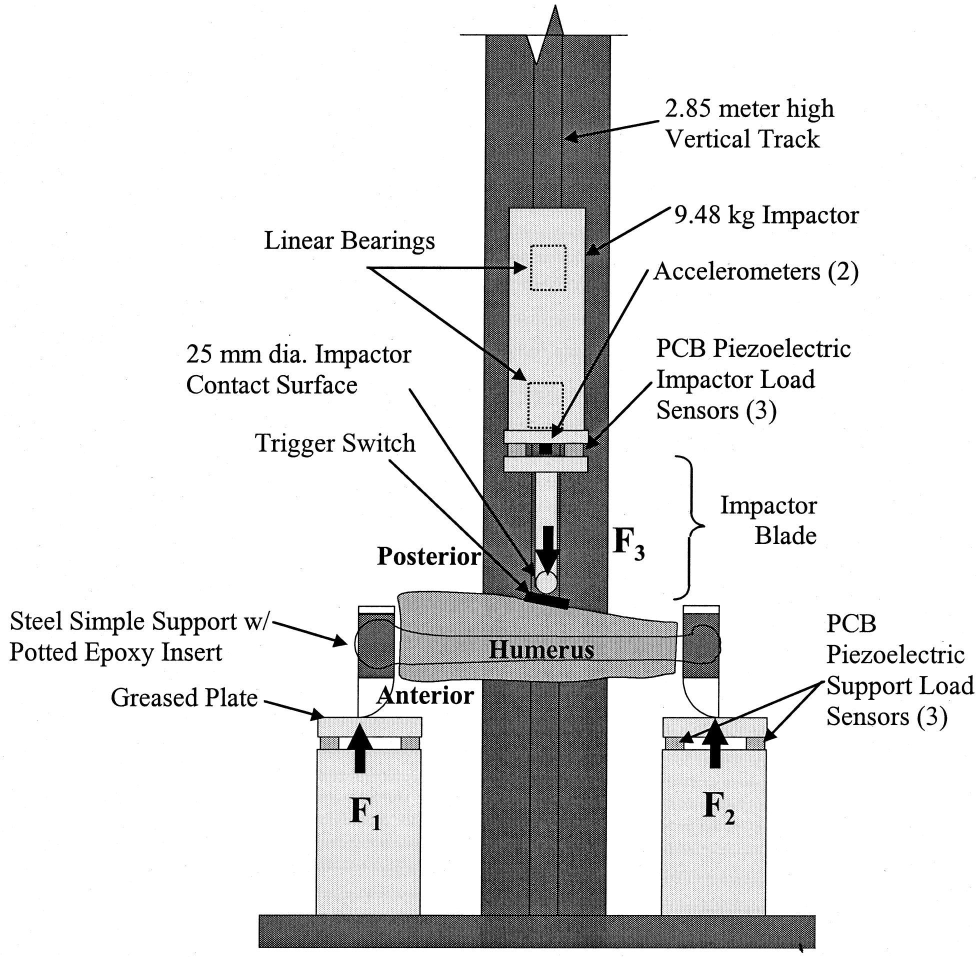

Fig. 2. Drop test configuration for the humerus tests.

ments, model CAE-13-125UN-350) were adhered midshaft on both the anterior and posterior sides of the humerus to provided maximum tensile and compressive strains. Pretest CT scans of each humerus were taken at 5 mm contiguous slices to determine bone cross-sectional properties. Pretest radiographs, both frontal and sagittal views, were taken to identify any pre-existing skeletal conditions. If any abnormal bone pathology was noticed, the specimen was removed from the test population. Post-test radiographs, both frontal and sagittal views, were taken and the humerus dissected to evaluate induced injury and classify fracture patterns.

Dynamic 3-point bending tests were performed using a 9.48 kg impactor released from a drop height of 1.35 m. The impactor was guided by a vertical linear bearing track which resulted in a pre-impact velocity of 3.63 m/s. This velocity was chosen to match humerus strain rates as measured in cadaveric subjects under side air bag loading. The humerus was impacted midshaft in the posterior-anterior direction as shown in Figure 2. This direction was chosen to correspond with the direction of humerus loading that would be seen from a deploying seat mounted side air bag. The impactor was brought to rest following fracture using a soft stop decelerator of crushable polystyrene. The proximal and distal simple supports each rested on greased plates. Each plate was supported by 3 quartz piezoelectric load sensors (PCB Piezotronics, model P212-B) aligned to measure force in the vertical direction. The impactor load was measured using 3 piezoelectric load sensors mounted in a similar fashion between the impactor blade and impactor mass. Accelerometers mounted to the impactor blade allowed for inertial compensation of the impact load. The initial contact between the impactor and the humerus was recorded by placing a conductive trigger switch on the humerus. Data were sampled at a rate of 20000 Hz, and filtered at SAE class 1000. High speed video (Kodak, model 1000-E, 1000 fps) recorded impactor displacement during the event.

Forearm tests

Ten female forearms were prepared by disarticulating the upper extremity at the shoulder and keeping the

Table 3. *Specimen information for female forearm tests*

T	SA	A	BM	CD
2.1	1013 left	64	49.9	Lung carcinoma
2.2	1013 right	64	49.9	Lung carcinoma
2.3	84 left	59	80.0	Adenocarcinoma of the lung
2.4	84 right	59	80.0	Adenocarcinoma of the lung
2.5	58 left	61	52.1	Bronchial carcinoma
2.6	58 right	61	52.1	Bronchial carcinoma
2.7	66 right	67	61.0	Respiratory failure
2.8	72 right	51	55.8	Ventricular failure
2.9	67 left	67	52.6	Respiratory failure
2.10	73 right	61	57.2	Myocardial infarction

T, test; SA, subject aspect; A, age (y); BM, body mass (kg); CD, cause of death.

elbow joint intact. As shown in Table 3, the average age of these specimens was 61 ± 5 y with an average body mass of 59.1 ± 11.6 kg. Simple mounts were designed to attach to the posterior side of the forearm via 2 tie wraps as shown in Figure 3. This mounting technique allowed for the forearm to be oriented in the supinated or pronated position before testing. The 3-point drop test device used for the humerus tests was again employed with the drop height adjusted to 2.0 m resulting in an impact velocity of 4.42 m/s. This velocity was chosen to match radius and ulna strain rates as measured in cadaveric tests with driver side air bags (Bass et al. 1997). In both the pronated and supinated positions, the upper extremity was positioned such that the impactor struck the anterior surface of the forearm. The impact location was established as the distal third of the forearm, which was taken as two-thirds of the ulna length measured distally from the olecranon. This location was chosen due to the local minimum polar moment of inertia of both the ulna and radius at the distal third of the forearm (Bass et al. 1997). Due to the lack of bone symmetry in the ulna and radius, strain gauge rosettes (Micro Measurements, model CAE-06-062UR-350) were used so that the principle strains could be determined. One rosette was placed at the distal third mark on both the posterior radius and posterior ulna. The 2-tailed Student's t test ($\alpha = 0.05$) was used to compare the data averages.

RESULTS AND DISCUSSION

Humerus tests

The results from the humerus dynamic 3-point drop tests are presented in Table 4. The average peak

Table 4. *Humerus dynamic 3-point drop test results*

TN	SA	AS	ASR	PS	PSR	PM	EM
1.1	79 right	1.14	1.26	−1.09	−1.34	167	21.0
1.2	79 left	1.24	1.33	−1.49	−1.34	177	19.7
1.3	75 right	2.21	3.69	−1.22	−2.86	127	29.0
1.4	75 left	2.91	5.48	−1.75	−4.48	153	24.0
1.5	78 right	1.25	3.87	−1.09	−3.37	156	22.2
1.6	78 left	2.10	4.57	−1.72	−5.25	170	28.2
1.7	82 right	1.14	3.74	−1.20	−3.69	113	31.5
1.8	82 left	1.18	4.74	−1.06	−4.15	139	24.3
1.9	81 right	2.65	3.36	−1.17	−4.70	146	21.5
1.10	81 left	Failed	Failed	−1.18	−5.12	134	19.3
1.11	80 right	1.68	4.76	−1.13	−2.88	216	26.5
1.12	80 left	1.06	3.96	Failed	Failed	147	26.3
Mean		1.69	3.70	−1.28	−3.56	154	24.5
S.D.		0.67	1.34	0.25	1.36	27	3.9

TN, test number; SA, subject aspect; AS, anterior strain (%); ASR, anterior strain rate (%/s); PS, posterior strain (%); PSR, posterior strain rate (%/s); PM, peak moment (Nm); EM, elastic modulus (GPa).

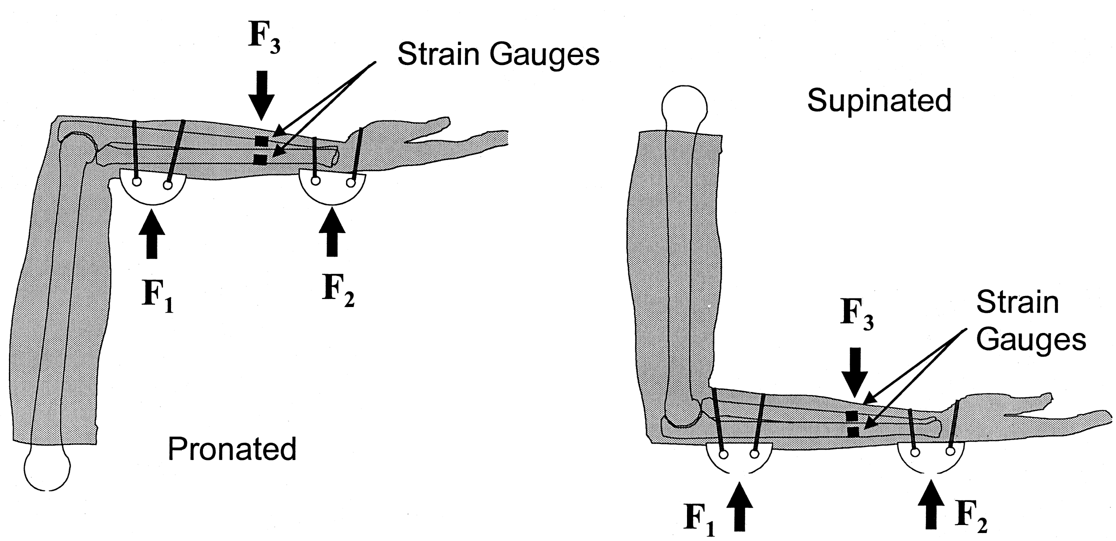

Fig. 3. Specimen preparation for the pronated and supinated forearm test configurations with the measured support loads shown as F_1, F_2, and the measured impactor load shown as F_3.

Table 5. *Supinated forearm dynamic 3-point drop test results*

T	SA	RPS	TRPS	RSR	UPS	TUPS	USR	PM	TPM
2.1	1013 left	1.180	4.7	6.78	0.889	5.2	9.94	87	4.9
2.4	84 right	1.170	8.5	4.40	1.175	8.6	4.84	92	8.7
2.5	58 left	1.640	7.1	4.10	0.757	7.8	4.30	96	7.5
Mean		1.330	6.8	5.10	0.940	7.2	6.36	92	7.0
s.d.		0.270	1.9	1.50	0.214	1.8	3.11	5	1.9

T, test; SA, subject aspect; RPS, radius peak strain (%); TRPS, time of radius peak strain (ms); RSR, radius strain rate (%/s); UPS, ulna peak strain (%); TUPS, time of ulna peak strain (ms); USR, ulna strain rate (%/s); PM, peak moment (Nm); TPM, time of peak moment (ms).

moment of 154 ± 27 Nm was mass scaled using the technique described by Eppinger et al. (1984) to produce the injury tolerance for the 5th centile small female humerus of 128 ± 19 Nm. Although this value was very similar to the 134 Nm presented by Kirkish et al. (1996), the similarity appears due to 2 opposing factors. The humeri in the study by Kirkish et al. were male and would tend to result in a higher value than female humeri; however, the tolerance was not scaled for dynamic testing, impact velocity of 0.22 m/s versus 3.6 m/s in the present study. Also, the relatively low standard deviation in the present study is a result of the close grouping of the small female sample population.

The average strain rates of 3.70 ± 1.34 %/s and -3.56 ± 1.36 %/s for the anterior and posterior gauges respectively highlighted the dynamic nature of the test and should be similar to humerus strain rates seen during side air bag loading. The strain gauge wire was broken during the event in the 2 tests that are marked as 'failed'. Using simple beam theory and ignoring shear effects, the average dynamic elastic modulus was found to be 24.5 ± 3.9 GPa. This was determined by plotting the stress, taken from the applied moment and cross-sectional bone properties, versus the strain directly measured from the in situ strain gauges. The slope of the linear region for each humerus was recorded for each test and averaged.

Forearm tests

Three matched pairs of forearms, tests 2.1 to 2.6, were tested with one forearm supinated and the other pronated to directly compare the differences. The results from all forearm tests are presented in Tables 5 and 6 separated by test condition. The instance of peak strain was noted as 'time' for all tests. The strain rates were calculated from the linear region before fracture from the strain time history plots. Within the 3 matched pair tests, the supinated position was significantly stronger ($P = 0.02$) than the pronated position with a 21 % higher average peak moment of 92 ± 5 Nm versus 75 ± 7 Nm respectively. Given this difference and the desire to produce a conservative injury tolerance, tests 2.7 to 2.10 were performed in the pronated position. Also, it is advantageous to choose this position given that typically the forearm is pronated while driving.

The average peak moment for the pronated forearms was 70 ± 13 Nm, and when mass scaled for the 5th centile female, the dynamic injury tolerance was determined to be 58 ± 12 Nm. This value agrees reasonably well with the results presented by Bass et al. (1997), who determined a forearm injury value of 67 ± 13 Nm as the 50 % risk of fracturing one bone in the forearm. This similarity suggests a preliminary validation of the biofidelity of the SAE instrumented upper extremity.

The average radius and ulna strain rates for the pronated tests were 3.64 ± 1.12 %/s and 2.70 ± 1.32 %/s respectively. The relatively high standard deviation for strain rates may be due to variability in the initial positioning of the strain gauges relative to the neutral axis, slight radius and ulna rotation during the impact, and the nonuniform geometry of the radius and ulna between specimens. There was no significant difference in radius and ulna strain rates between the 2 positions. The strain rates compare well to rates recorded for air bag loading which ranged from 1.3 to 5.3 %/s. The difference in loading between the pronated and supinated positions was investigated in more detail by examining the impact time histories as well as the forearm fracture patterns and locations.

Forearm impact time histories

The in situ strain gauges were used to determine not only peak strain and strain rate, but also the fracture

Table 6. *Pronated forearm dynamic 3-point drop test results*

T	SA	RPS	TRPS	RSR	UPS	TUPS	USR	PM	TPM
2.2	1013 right	0.775	4.8	4.50	0.568	3.0	4.50	69	4.7
2.3	84 left	1.160	11.5	3.24	0.525	7.9	1.85	82	11.4
2.6	58 right	1.830	9.2	2.05	0.606	4.0	4.74	74	9.2
2.7	66 right	1.240	6.5	4.09	0.241	3.7	1.24	48	6.5
2.8	72 right	1.880	8.9	2.54	0.156	4.5	1.40	83	9.0
2.9	67 left	0.961	5.3	5.62	0.393	2.5	3.00	58	5.6
2.10	73 right	1.280	8.5	3.45	0.286	4.2	2.17	73	8.6
Mean		1.300	7.8	3.64	0.396	4.3	2.70	70	7.8
S.D.		0.380	2.2	1.12	0.162	1.6	1.32	13	2.2

T, test; SA, subject aspect; RPS, radius peak strain (%); TRPS, time of radius peak strain (ms); RSR, radius strain rate (%/s); UPS, ulna peak strain (%); TUPS, time of ulna peak strain (ms); USR, ulna strain rate (%/s); PM, peak moment (Nm); TPM, time of peak moment (ms).

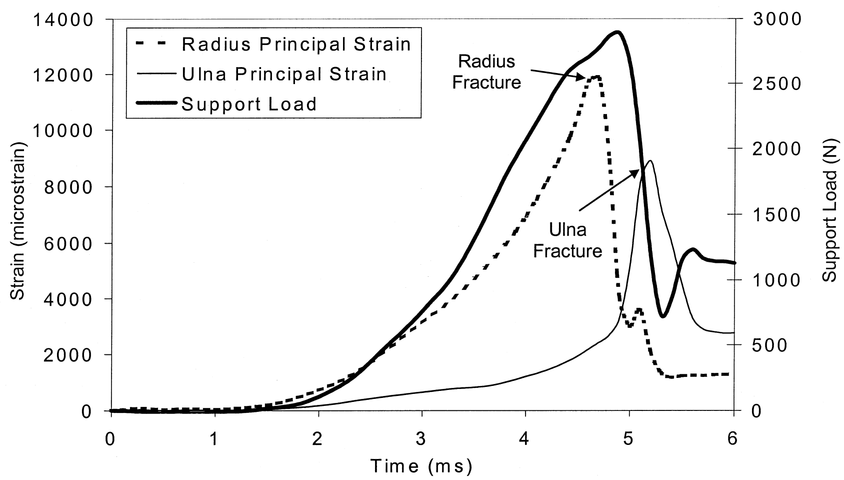

Fig. 4. Strain and support load time history for the supinated test 2.1.

times of the radius and ulna. Since the trigger time depended on the amount of soft tissue and trigger strip placement for each test, the time history plots could only be used as a relative measure of fracture time within each test. In the supinated position the average difference in fracture time between the radius and ulna was a negligible 0.4 ± 0.3 ms. However, the pronated tests yielded an average difference in fracture time of 3.6 ± 1.2 ms, with the ulna breaking before the radius in every test. This difference is significant ($P = 0.0001$) for comparing only the matched pairs, and significant ($P = 0.05$) for all tests. As illustrated in Figures 4 and 5, this trend implies that in the pronated position, the ulna and radius are loaded independently, while in the supinated position the ulna and radius are loaded together as a combined structure. These 2 figures also highlight the difference in peak strain values between the 2 positions. While the average radius peak strains for supinated and pronated tests were similar at 6.8 ± 1.9% and 7.8 ± 2.2% respectively. The average ulna peak strains were significantly different ($P = 0.03$) and 7.2 ± 1.8% for the supinated tests and 4.3 ± 1.6% for the pronated tests. Furthermore, in pronation the peak strain for the ulna was significantly less ($P = 0.0007$) than the peak strain in the radius.

Forearm fracture analysis

The post-test x-rays were used to assess fracture pattern and location. Measurements were taken to assess relative fracture locations using midfracture points. The distance from the olecranon or radial head to the midfracture point was expressed as a percentage of the bone's total length. This technique allowed us to compensate for radiographic magnification and compare fracture location. The distance between the radius and ulna fracture was determined

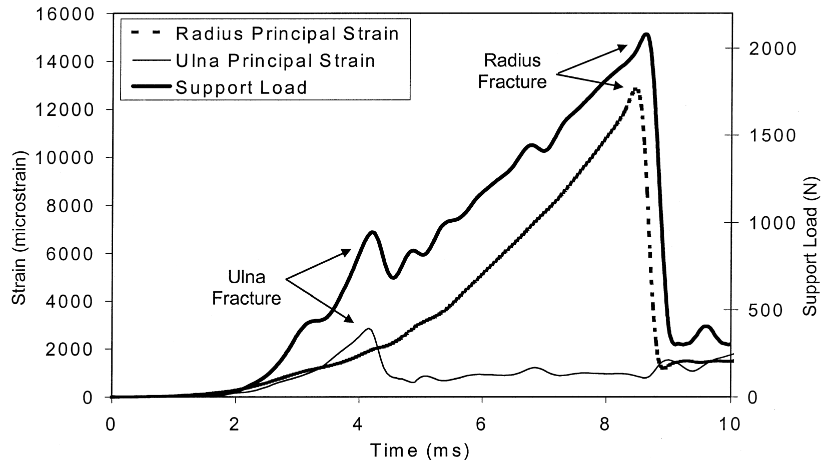

Fig. 5. Strain and support load time history for the pronated test 2.10.

Table 7. *Supinated forearm fracture results*

T	UFL	RFL	UFRF	UFP	RFP
2.1	68	60	−1.6	B2-butterfly	A3-transverse
2.4	78	58	−12.8	A2-oblique	A3-transverse
2.5	77	60	−12.8	A2-oblique	B2-butterfly
Mean	74	59	−9.1		
S.D.	6	1	6.5		

T, test; UFL, ulna fracture location (%); RFL, radius fraction location (%); UFRF, ulna fracture to radius fracture (%); UFP, ulna fracture pattern; RFP, radius fracture pattern; B2, butterfly by bending with 2 segments; A2, oblique; A3, transverse.

* Distance measured distally from the ulna fracture to the radius fracture expressed as a percentage of ulna length. A negative value denotes a radius fracture that is proximal to the ulna fracture.

Table 8. *Pronated forearm fracture results*

T	UFL	RFL	UFRF	UFP	RFP
2.2	66	63	10.7	A2-oblique	A3-transverse
2.3	72	67	0.4	A3-transverse	B2-butterfly
2.6	69	61	−2.7	B2-butterfly	B2-butterfly
2.7	72	63	−9.0	A2-oblique	B2-butterfly
2.8	68	62	1.7	A2-oblique	B2-butterfly
2.9	69	66	3.8	B2-butterfly	B2-butterfly
2.10*	85	68	−11.7	A2-oblique	A2-oblique
Mean	72	64	−1.0		
S.D.	6	3	7.6		

T, test; UFL, ulna fracture location (%); RFL, radius fraction location (%); UFRF, ulna fracture to radius fracture (%); UFP, ulna fracture pattern; RFP, radius fracture pattern; A2, oblique; A3, transverse; B2, butterfly by bending with 2 segments.

* Previous healed proximal fracture of the radius and ulna, new fracture occurred distal to the old fracture site.

and expressed as a percentage of the ulnar length. Table 7 details the supinated tests while Table 8 contains the pronated tests.

The fracture patterns were confirmed with necropsies of each forearm. No evidence of disruption was seen at the proximal and distal radioulnar joints. The fracture pattern was documented using the classification system devised by Johner & Wruhs (1983) to describe tibial fractures. This system classifies according to the fracture pattern and the likely fracture mechanism: A1 = spiral; A2 = oblique; A3 = transverse; B1 = butterfly fragment by torsion; B2 and B3 = butterfly by bending with one or several fragments respectively; C1 = comminuted by torsion; C2 = segmental; C3 = crush. While the majority of the radius fractures in the pronated position were of the B2 butterfly type, no obvious fracture pattern trends were seen.

The forearm was impacted at a point that would correspond to a percentage of total ulna length of 66 %. In both groups the ulna fracture occurred distal to this point, $74 \pm 6\,\%$ in the supinated position and $72 \pm 6\,\%$ in the pronated position. However, the relationship of ulna fracture to the radius fracture between the supinated and pronated groups was different. In the supinated group the radius fracture occurred proximal to the ulna fracture with an average distance of $-9.1 \pm 6\,\%$, while in the pronated group, the average distance between fractures was $-1.0 \pm 7.6\,\%$. While this difference was not significant ($P = 0.09$) it did indicate a trend. These results suggest variability in the fracture location depending on whether the forearm was supinated or pronated. This variability was also evident when comparing the average fracture locations for each bone separately. The radius fracture location was significantly ($P = 0.003$) more proximal, $59 \pm 1\,\%$ versus $64 \pm 3\,\%$, in the supinated group versus the pronated group. Although the ulna fracture location seemed more distal, $74 \pm 6\,\%$

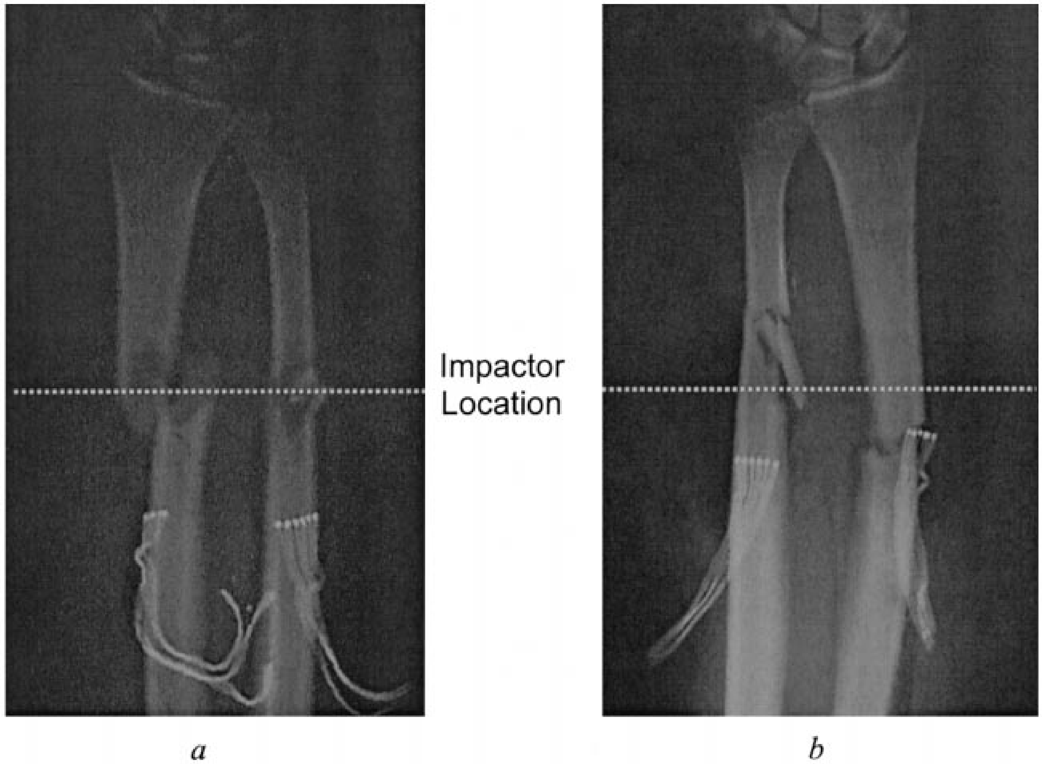

Fig. 6. Comparison of the pronated fracture location for forearm tests 2.3 (*a*) versus the matched supinated fracture location for test 2.4 (*b*). The strain guages and wiring can be seen proximal to the impactor location on both bones for both tests.

versus $72 \pm 6\%$, in the pronated group versus supinated group, this comparison was not significant ($P = 0.52$). These observations were confirmed by direct comparison of the matched pair x-rays as shown in Figure 6.

These results suggest that the radius and ulna were being loaded sequentially in the pronated arm and the subsequent fractures were occurring directly beneath the impactor head. The ulna was loaded and failed before the radius was appreciably loaded. In the supinated position the impact force was more evenly distributed between the 2 bones. The tendons and muscle bellies of the forearm flexor compartment helped distribute the impactor load in the supinated position, whereas in the pronated position the ulna was relatively exposed. The difference in fracture location suggests that the supinated forearms fractured at weaker points rather than directly underneath the impactor as in the pronated forearms.

CONCLUSIONS

The dynamic bending strength of the 5th centile female humerus was determined to be 128 Nm. It is anticipated that this value will be used for investigations of side air bag loading of the female humerus. The dynamic elastic modulus for the female humerus was found to be 24.4 GPa and should prove useful for finite element modelling of the humerus.

For use with driver-side air bag studies, the female forearm injury tolerance was investigated. Drop tests using matched pairs of female upper extremities revealed that the forearm is 21% stronger in the supinated position. The fracture location for the pronated tests occurred directly under the impactor, while in the supinated tests the radius fractures more proximal and the ulna more distally than in the pronated position. Given that the forearm is typically pronated in the driving position and the desire to produce a conservative injury criterion, the weaker pronated position was used and scaled to give the dynamic bending strength of the 5th centile female forearm of 58 Nm.

The similarity between the presented forearm injury criterion of 58 Nm for the female cadaver and that found by Bass et al. (1997) of 67 Nm for the SAE upper extremity suggests a preliminary biofidelity validation. The higher dummy response was most likely due to the fact that the SAE upper extremity is slightly more massive than the reference 5th centile female. While no discussion of the dummy's kinematic biofidelity was given, it is suggested that the SAE upper extremity tends to overestimate the forearm loads and thus provides a conservative estimate of the injury potential.

REFERENCES

BASS CR, DUMA SM, CRANDALL JR, MORRIS R, MARTIN P, PILKEY WD et al. (1997) The interaction of air bags with upper extremities. Paper number 973324. Warrendale, Pennsylvania: Society of Automotive Engineers

CARTER DR, CALER WE (1983) Cycle-dependent and time-dependent bone fracture with repeated loading. *Journal of Biomechanical Engineering* **105**, 166–170.

EPPINGER RH, MARCUS JH, MORGAN RM (1984) Development of dummy and injury index for NHTSA's thoracic side impact protection research program. Paper number 840885. Warrendale, Pennsylvania: Society of Automotive Engineers.

JOHNER R, WRUHS O (1983) Classification of tibial shaft fractures and correlation with results after rigid internal fixation. *Clinical Orthopaedics and Related Research* **178**, 7–25.

KALLIERIS D, RIZZETTI A, MATTERN R, JOST S, PRIEMER P, UNGER M (1997) Response and vulnerability of the upper arm through side air bag deployment. Paper number 973323. Warrendale, Pennsylvania: Society of Automotive Engineers.

KIRKISH SL, BEGEMAN PC, PARAVASTHU NS (1996) Proposed provisional reference values for the humerus for evaluation of injury potential. Paper number 962416, Warrendale, Pennsylvania: Society of Automotive Engineers.

KUPPA SM, YEISER CW, OSLON MB, TAYLOR L, MORGAN R, EPPINGER R (1997) RAID – An investigation tool to study air bag/upper extremity interactions. Paper number 970399. Warrendale, Pennsylvania: Society of Automotive Engineers.

MESSERER O (1880) *Über Elasticität und Festigkeit der menschlichen Knochen*. Stuttgart: J. G. Cotta'schen Buchhandlung.

NATIONAL HIGHWAY TRAFFIC SAFETY ADMINISTRATION (1996) *Third Report to Congress: Effectiveness of Occupant Protection Systems and Their Use*, pp. 24–25. Washington D.C.: U.S. Department of Transportation.

WEBER C (1859) *Chirurgische Erfahrungen und Untersuchungen*, pp. 171–174.